U. S. DEPARTMENT OF COMMERCE
NATIONAL OCEANIC AND ATMOSPHERIC ADMINISTRATION
NATIONAL METEOROLOGICAL CENTER

OFFICE NOTE #372

PRELIMINARY RESULTS OF THE FINITE ELEMENT PARALLEL RUN 6/20/1990 TO 7/1/1990

J. STEPPELER

AND

M. IREDELL

JULY 1990

THIS IS AN UNREVIEWED MANUSCRIPT, PRIMARILY INTENDED FOR INFORMAL EXCHANGE OF INFORMATION AMONG NMC STAFF MEMBERS.

1. The finite element scheme

For the parallel run the finite element scheme was introduced for the vertical advection terms only. The fields q,U,V,T are represented by amplitudes $q_\nu, U_\nu, V_\nu, T_\nu$ on full model levels σ_ν. The vertical velocity $\dot{\sigma}$ is represented by amplitudes $\dot{\sigma}_{\nu+1/2}$ on half levels $\sigma_{\nu+1/2}$. The approximation equations will be given for q as an example. The representation by basis functions is assumed to be by linear splines for q and by piecewise constant basis functions for $\dot{\sigma}$.

$$q(\sigma) = \sum q_\nu \, e_\nu(\sigma)$$

$$\dot{\sigma}(\sigma) = \sum \dot{\sigma}_{\nu+1/2} \, b_{\nu+1/2}(\sigma)$$

with $e_\nu(\sigma)$ being linear for $\sigma \neq \sigma_\nu$ and

$$e_\nu(\sigma_\nu)=1 \text{ and } e_\nu(\sigma_\mu)=0 \text{ for } \nu\neq\mu \ , \qquad (1)$$

$$b_{\nu+1/2}(\sigma) = 1 \text{ for } \sigma_\nu < \sigma < \sigma_{\nu+1}, \ b_{\nu+1/2}(\sigma) = 0 \text{ otherwise}$$

The equation to be approximated is the advection part of the dynamic equation

$$\dot{q} = \dot{\sigma}\, q_\sigma \qquad (2)$$

It is approximated using a least square principle with the functional representation of eq.(1). The $\dot{q}_\nu$ are determined by the functional equation

$$\partial R/\partial \dot{q}_\nu = 0, \qquad (3)$$

with $R = \int (\dot{q} - \dot{\sigma}\, q_\sigma)^2 w(\sigma) d\sigma$, and q and σ being given by eq.(1). The positive weight function $w(\sigma)$ is determined such that the

approximation to eq.(2) remains second order accurate even for irregular grids. This is achieved by choosing the same piecewise constant functional representation for $w(\sigma)$ as for σ, with

$$w(\sigma_{v+1/2}) = 1/(\sigma_{v+1} - \sigma_v)^2 \qquad (4)$$

The accuracy of advection is considerably improved compared to the operational scheme, which is only first order on irregular grids. For regular grids the operational scheme is second order accurate and the finite element scheme has a fourth order accuracy.

This higher order scheme has a lower critical CFL number and would therefore require a reduced timestep for cases of very strong vertical velocity. However, with the present operational timestep there is no danger of numerical instability for this reason, since the CFL number is checked during the integration. If it exceeds a critical value , these gridpoints are computed by the operational scheme. In the present parallel run the theoretical critical CFL number of .7 has not been reached, even though the forecast has on occasions come close to this value.

2. Results

The parallel run started on 1990/6/16-0Z. The finite element model was used for 6 hour first guesses in the assimilation system as well as for 10 day forecasts from 0Z each day. First, the system was run for 4 days for the advection of moisture only. This moisture only scheme had only a

small impact in terms of the 500mb and 1000mb height fields. At day 5 the correlation between the parallel and operational runs was greater than 99%. The full finite element scheme was introduced on 6/19-12Z. A small reduction of the first guess error of height could then be observed, as shown in fig.1. Consistent with previous experience most relevant changes occur after day 5. However, some differences can be observed earlier. Fig 2a,b show the rainfall at 48 hr for the finite element and the operational run starting at 90/6/25. There is a very great similarity between the two forecasts in respect to the rainfall patterns. The amplitudes, however, show rather significant differences. This is reflected in differences of the globally averaged precipitation, as shown in fig. 3, which gives the global precipitation as a function of forecast time for the forecasts starting 90/6/25. The finite element forecast has a more constant rainfall rate than the operational run. Fig. 4 shows the same diagram for the forecast starting 90/6/28, which displays a similar difference between the two model versions.

There have been two occurrences of significant differences in short range forecasts. Fig. 5 shows the two day surface pressure forecast starting 90/6/21 and fig.6 gives the corresponding forecast for the MRF model. The main difference concerns the low over the east coast of the USA, which is predicted 4 mb deeper by the finite element model. Also, the finite element model produces only one center of the low, whereas the MRF forecast has two centers. The one day MRF forecast verifying on the same day is shown in fig.7. It supports the 48hr finite element forecast in producing also only one center of the low. The verification of the limited area analysis is shown in fig. 8. it is in good agreement with the 48 hr finite element forecast.

Fig. 9 shows the 48 hr forecast starting 90/6/28, and fig 10 gives the same forecast for the MRF model. The main difference is the position of

the low over central USA, which is more to the northeast with the finite element forecast. The 24 hr MRF forecast , shown in fig. 11, agrees with the 48 finite element forecast, in connecting this low with that in the north Atlantic. The verifying analysis , given in fig. 12 confirms the more north westerly position of this low.

The five day forecasts starting 1990/6/28, shown in fig. 13 for the finite element forecast and in fig.14 for MRF, differ quite substantially. The verifying analysis is given in fig. 15. The main difference is the strongly developed Atlantic low forecasted by the MRF, which is forecasted much weaker by the finite element model, in accordance with the verifying analysis. There are also differences in the forecast of the complex low over central USA and that on the east coast, as well as the ridge near 90^0 west. There is more indication of the last two features in the finite element forecast than with the MRF model. There are more differences between the two forecasts, which indicate a greater sensitivity of the MRF model to the finite element discretisation than previously experienced in the ECMWF model. This increased sensitivity is consistent with the results of experiments done before the parallel run.

Five day verifications are available from 6/20 to 7/1. The anomaly correlations of height for the northern hemisphere are shown in fig. 16 for 1000mb and 500mb. There is an average increase of skill of 2% at 1000mb and of 0.3% at 500mb. For the southern hemisphere the scores were negative on the average. However, there was a great spread in these forecasts, and the sample is too small to obtain a significant result. The effect of the finite elements on the mean error of the lower levels was not systematic. However, at 200mb the MRF model shows consistently negative mean errors of height. This feature was systematically improved by the finite elements. Table 1 gives the mean error of height at day 5 for the MRF and finite element models. There is a considerable reduction of

this error for every day of the assimilation. The same is true for the southern hemisphere, even for days where the anomaly correlations are worse with the finite elements than for the MRF.

Date	MRF	finite elements
6/20	-19.5	-10.6
6/21	-19.2	- 8.5
6/22	-19.3	- 9.1
6/23	-26.3	-17.5
6/24	-19.1	-12.8
6/25	-19.2	-11.6
6/26	-22.5	-15.2
6/27	-27.2	-17.6
6/28	-36.9	- 7.8
6/29	-22.1	-13.0
6/30	-26.9	-15.3
7/01	-23.4	-15.4

Table1 Mean errors of height , northern hemisphere at 200mb.

List of figures:

fig.1: First guess error of height against radiosondes, pry: finite elements, MRF, operational

fig.2: Rainfall for the 48 hr forecast staring 1990/6/25, a, MRF b, finite elements

fig.3: Globally averaged rainfall for forecast from 1990/6/25 as function of time for forecast from1990/6/25 .

fig.4: As fig. 4, for forecast starting 1990/6/28.

fig.5 48 hr forecast of surface pressure for the finite element model, starting 1990/6/21 :

fig.6: As fig.5, for the MRF model.

fig.7: 24 hr forecast of surface pressure of the MRF model, starting 1990/6/22 :

fig.8: Verifying limited area analysis for figs5,6,7.

fig.9: 48 hr forecast of surface pressure for the finite element model, starting 1990/6/28 :

fig.10: As fig.9, for the MRF model.

fig.11: 24 hr forecast of surface pressure of the MRF model, starting 1990/6/29 .

fig.12: Verifying analysis for figs. 9,10,11.

fig.13: 120 hr forecast of surface pressure for the finite element model, starting 1990/6/28 :

fig.14: As fig.13, for the MRF model.

fig.15: Verifying analysis for figs. 13,14.

fig.16: Difference of anomaly correlations of height of finite element minus MRF model for 1000mb and 500mb and averaged values for the period 1990/6/20 to 1990/7/1.

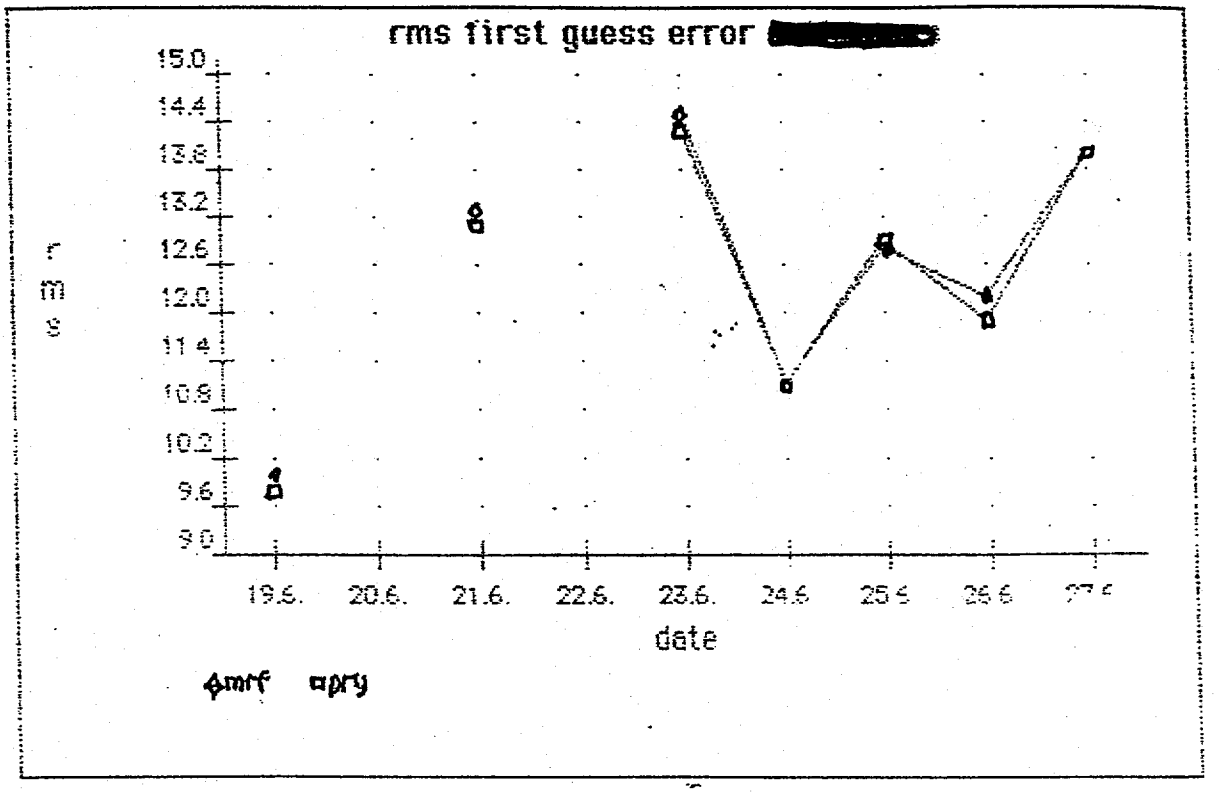
rms first guess error [redacted]
15.0
14.4
13.8
13.2
12.6
12.0
11.4
10.8
10.2
9.6
9.0
rms
19.6.
20.6.
21.6.
22.6.
23.6.
24.6
25.6
26.6
date
mrf
pry

Fig 1

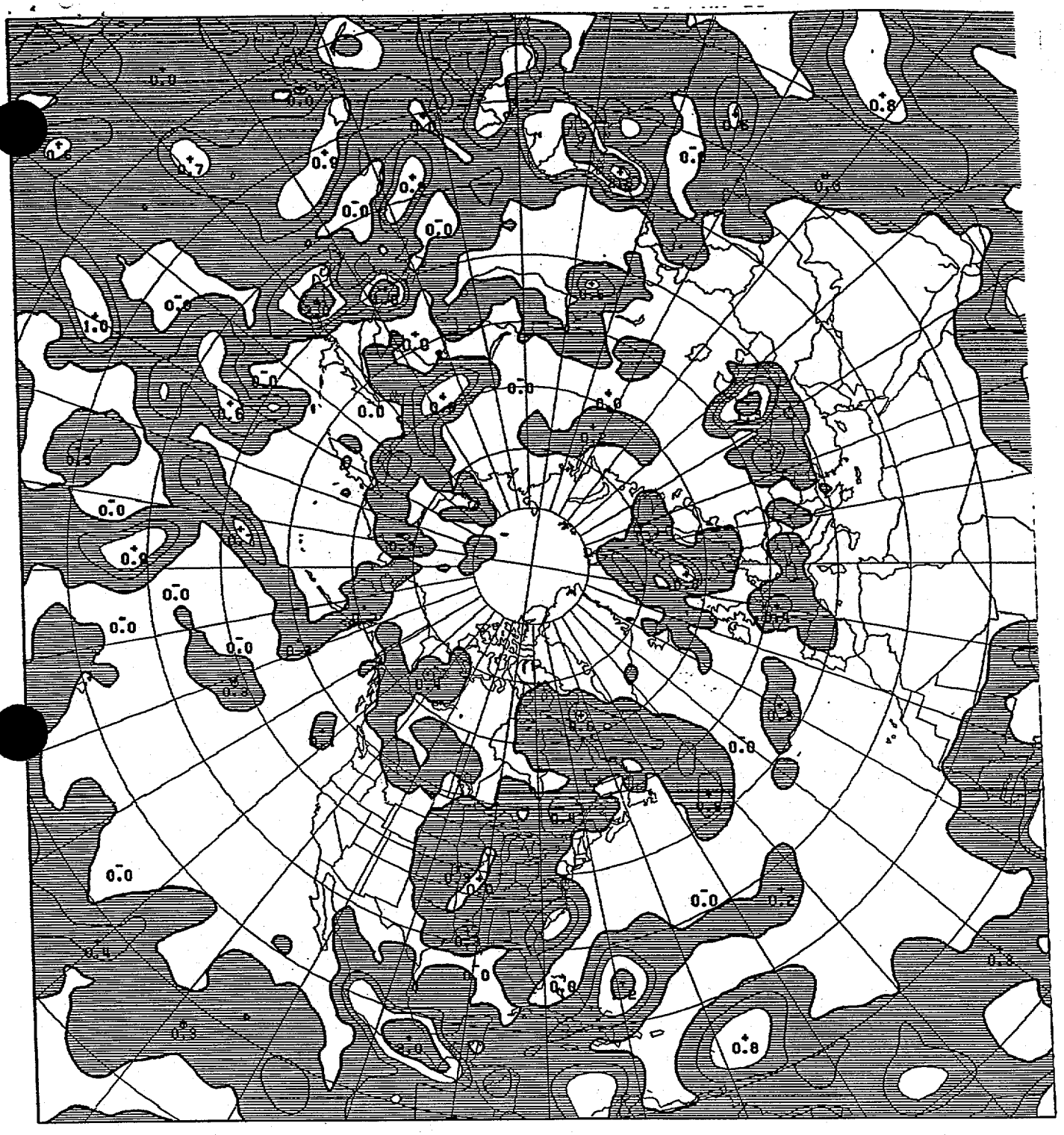

Fig 2a

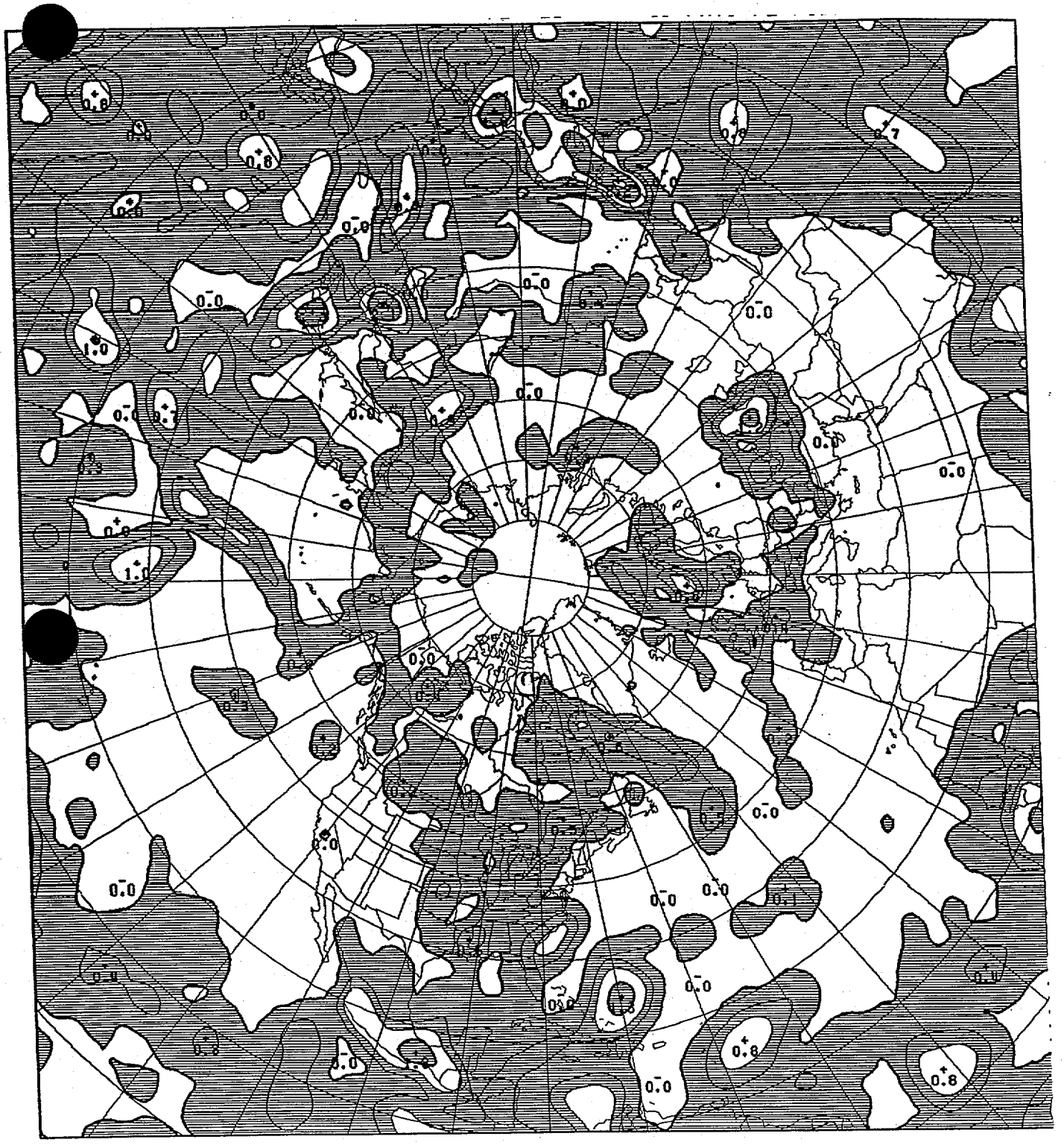

Fig 2 b

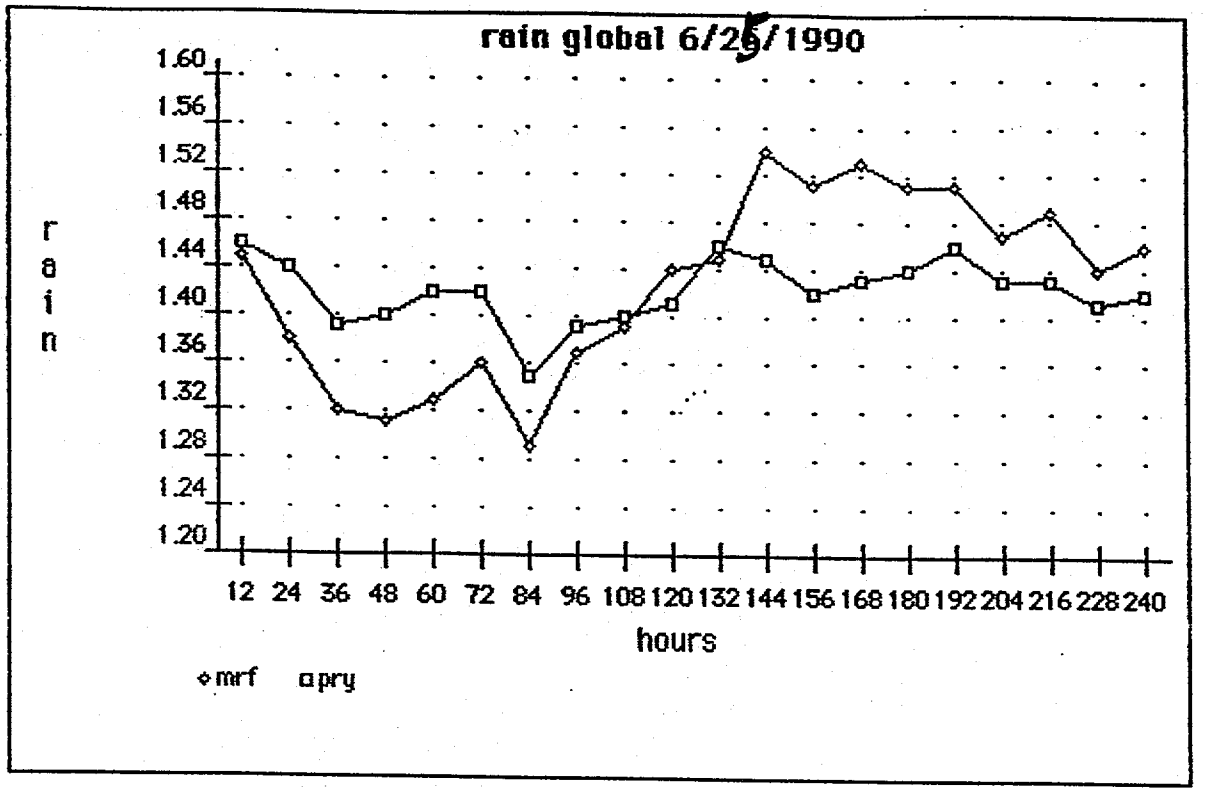
rain global 6/25/1990
1.60
1.56
1.52
1.48
1.44
1.40
1.36
1.32
1.28
1.24
1.20
rain
12 24 36 48 60 72 84 96 108 120 132 144 156 168 180 192 204 216 228 240
hours
mrf
pry

Fig 3

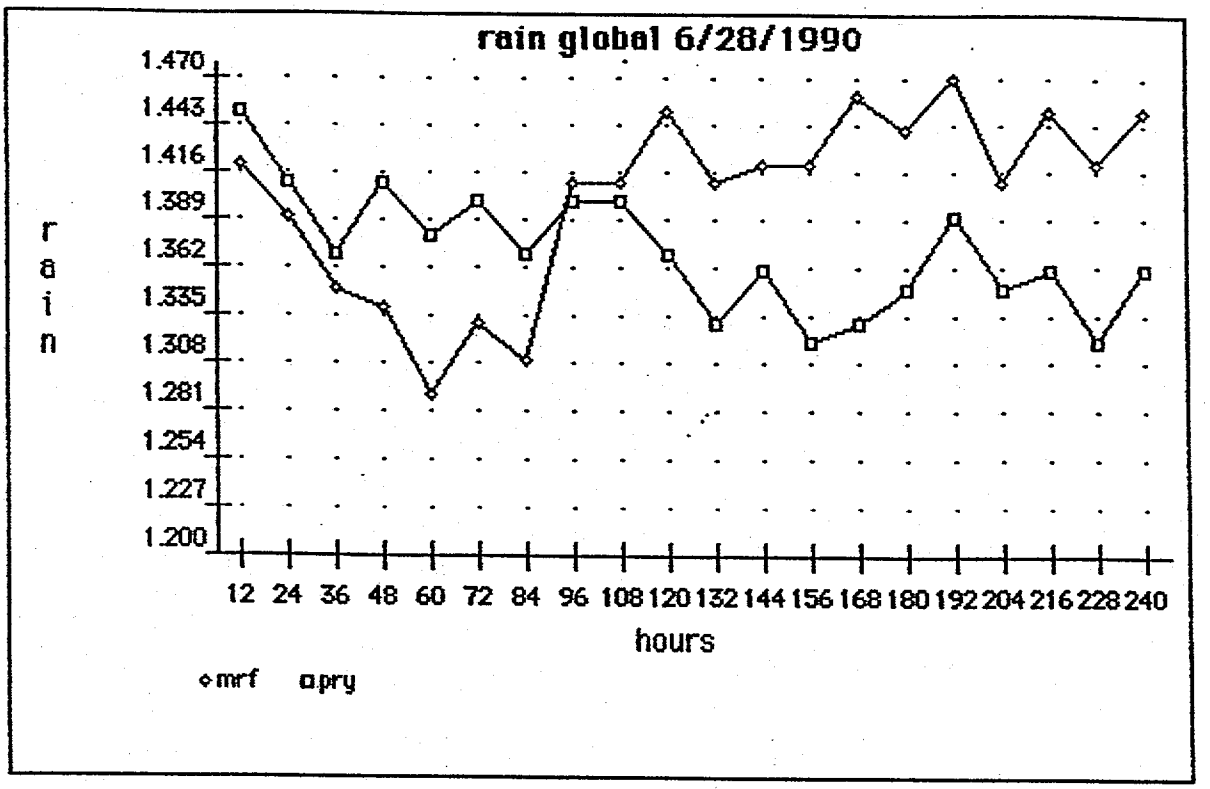
rain global 6/28/1990
1.470
1.443
1.416
1.389
1.362
1.335
1.308
1.281
1.254
1.227
1.200
rain
12 24 36 48 60 72 84 96 108 120 132 144 156 168 180 192 204 216 228 240
hours
mrf
pry

Fig 4

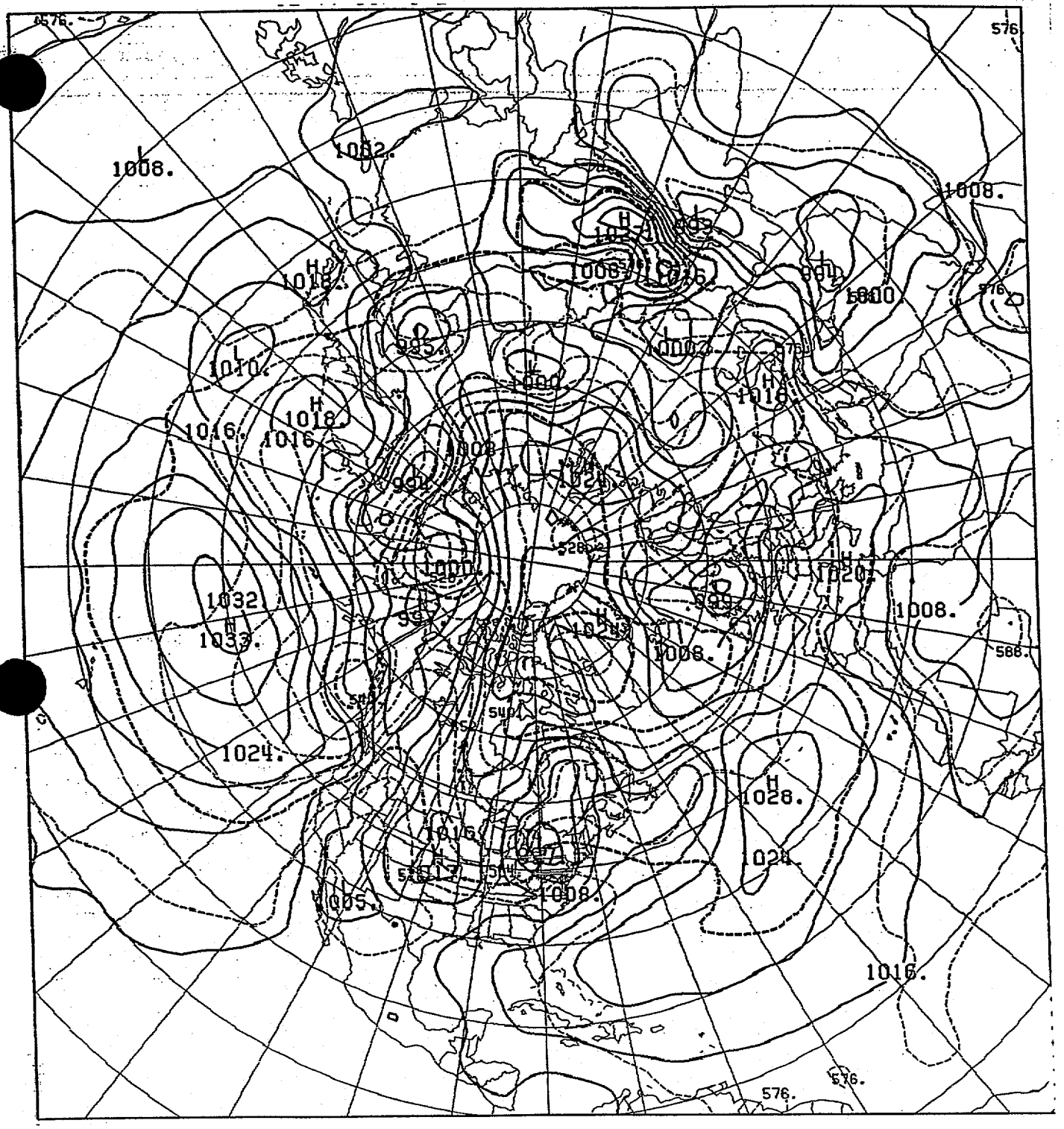
576.
576
1008.
1002.
1008.
1018.
1010.
1016.
1018.
1016.
1032
1033.
1024.
1008.
1008.
1020.
1008.
1028.
1024.
1016.
1008.
1016.
576.
576.

Fig 5

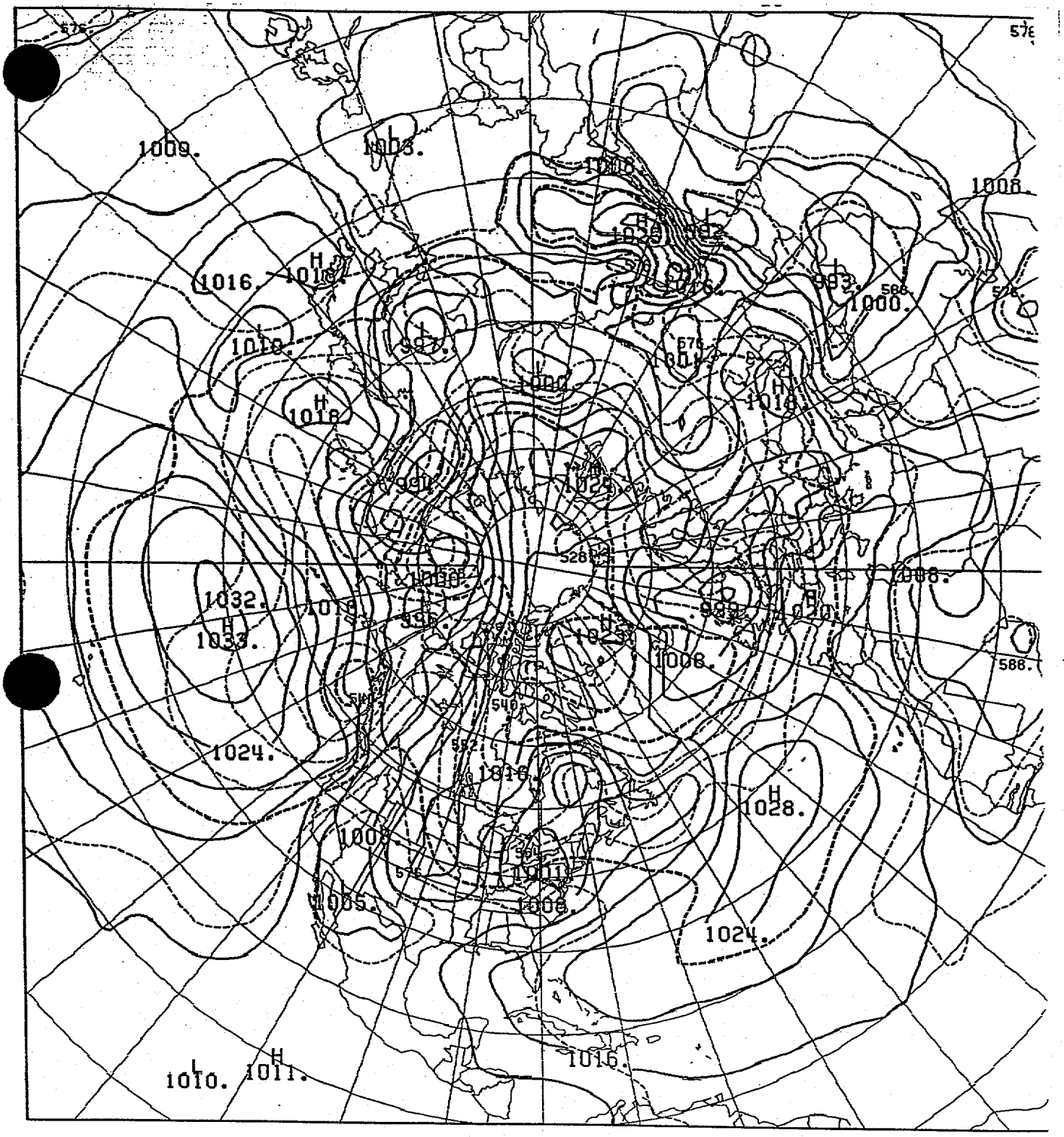
1009.
1003.
1008.
1016.
1018.
1010.
997.
1000.
1018.
994.
1024.
1032.
1033.
1018.
996.
1023.
1008.
1008.
588.
1024.
1016.
1028.
1008.
1005.
1008.
1024.
1016.
1010.
1011.

Fig 6

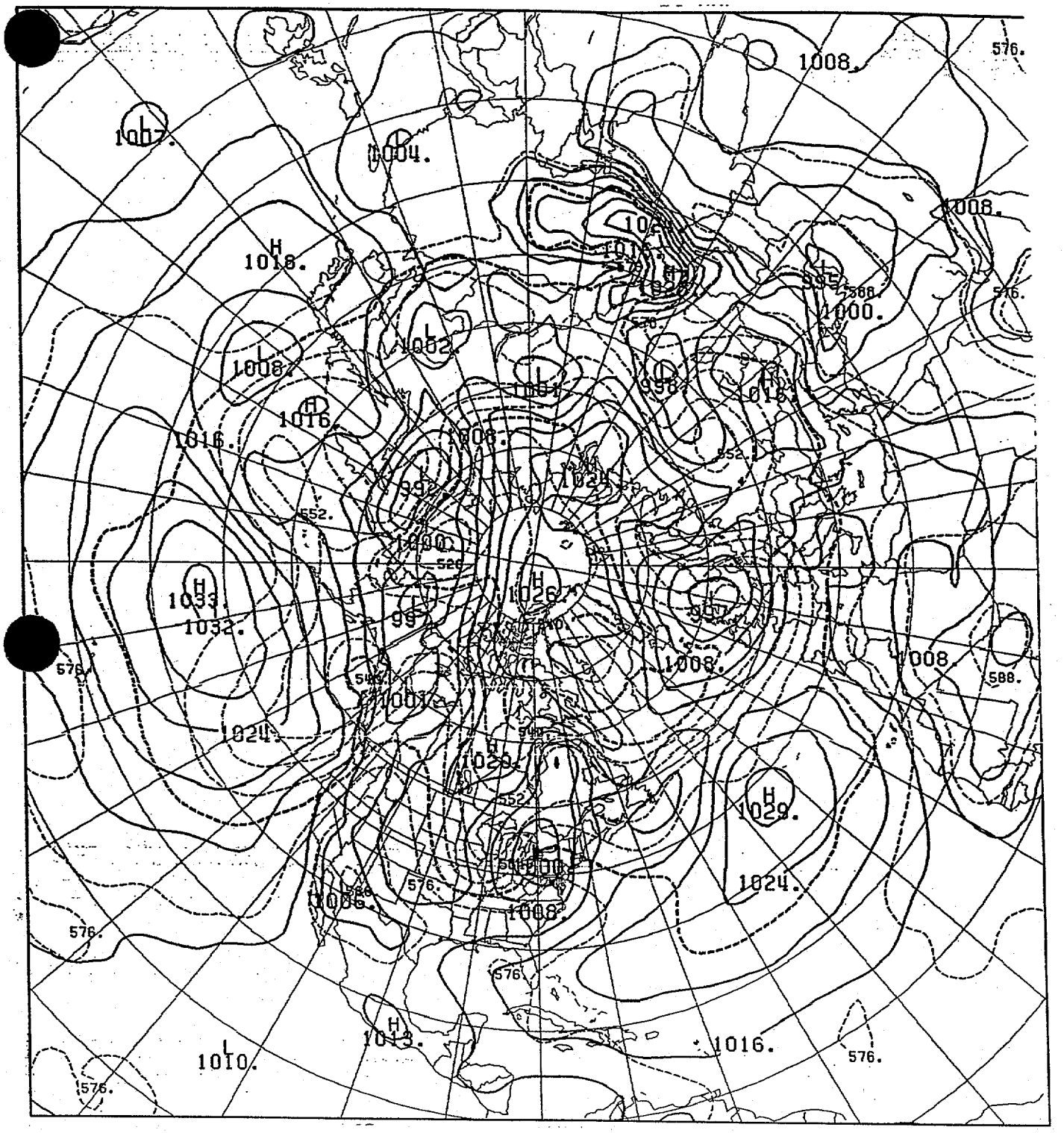
1008.
576.
1007.
1004.
1008.
1018.
1000.
1002.
1008.
1016.
1016.
1008.
552.
1000.
1033.
1032.
1026.
1008.
1008.
588.
576.
1001.
1024.
1029.
1024.
1006.
1008.
576.
576.
1013.
1016.
1010.
576.
576.

Fig 7

MSL PRESSURE (MB) ------- VALID 00Z SAT 23 JUN 1990
1000-500MB THKN (DAM) --- VALID 00Z SAT 23 JUN 1990

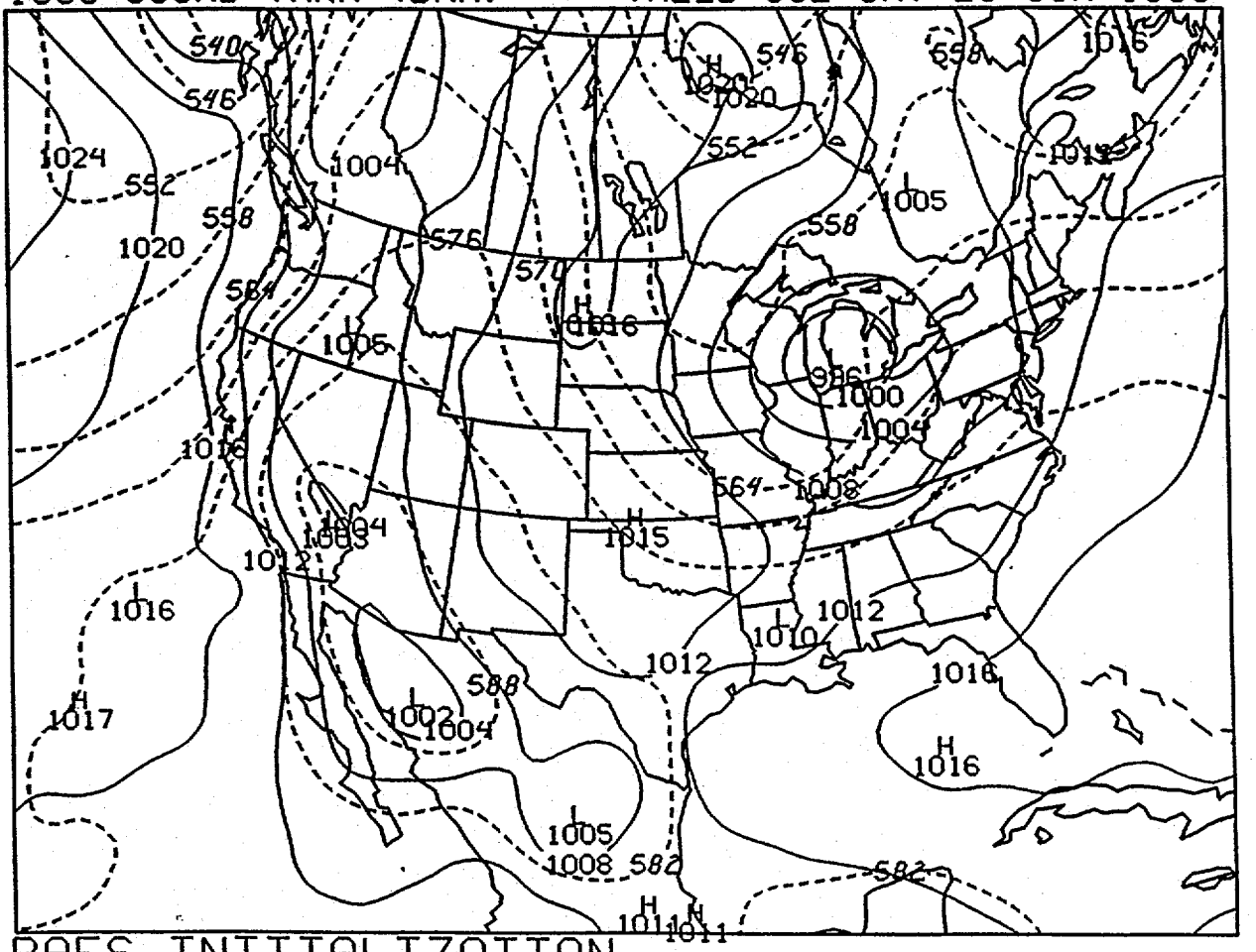

RAFS INITIALIZATION

Fig 8

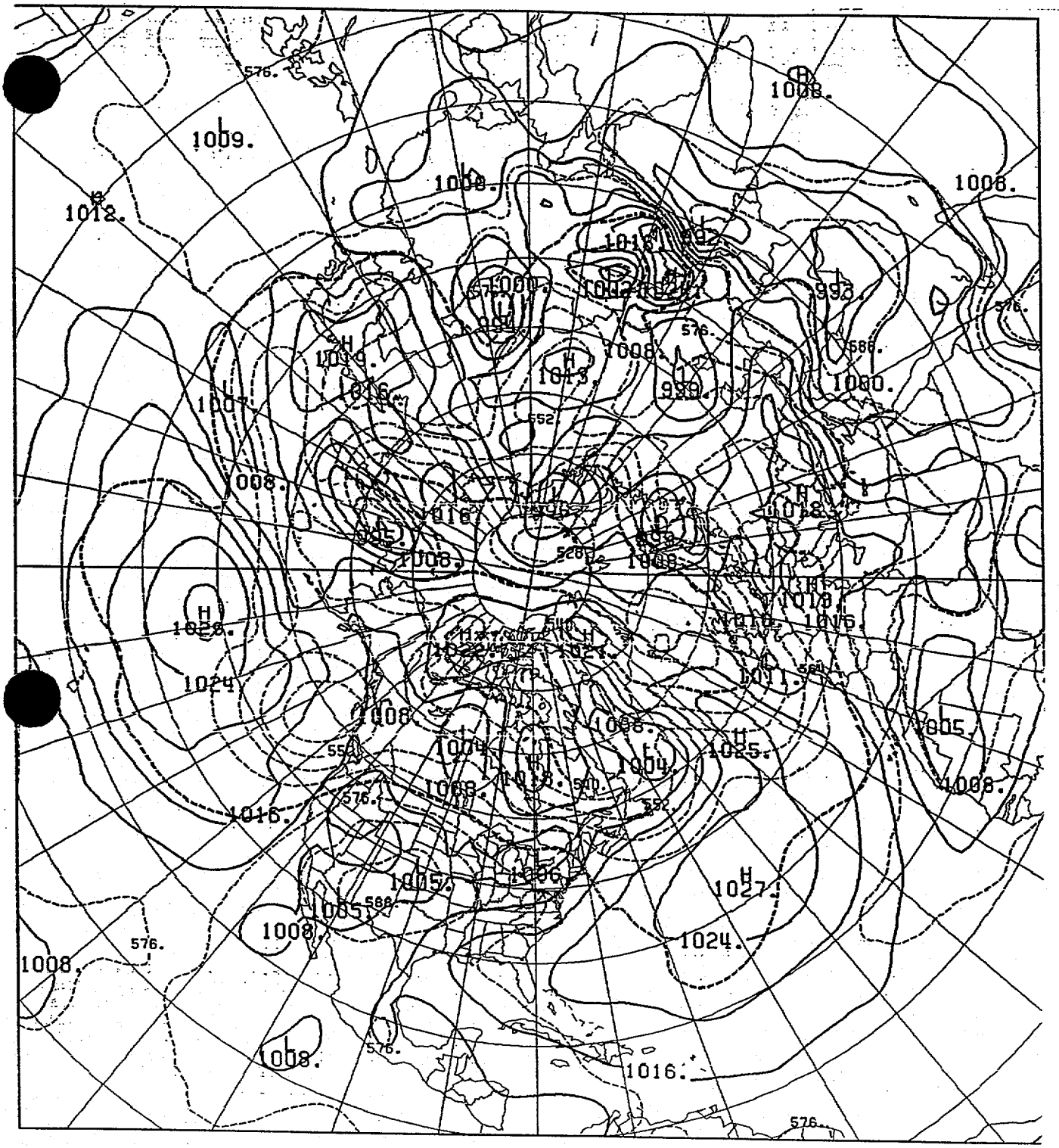
1009.
1012.
1008.
1006.
1000.
1007.
1008.
1016.
1024.
1025.
1027.
1005.
1004.
1011.
1019.
1013.
1018.
1020.
1021.
1022.
576.
588.
552.
528.
540.
564.

Fig 9

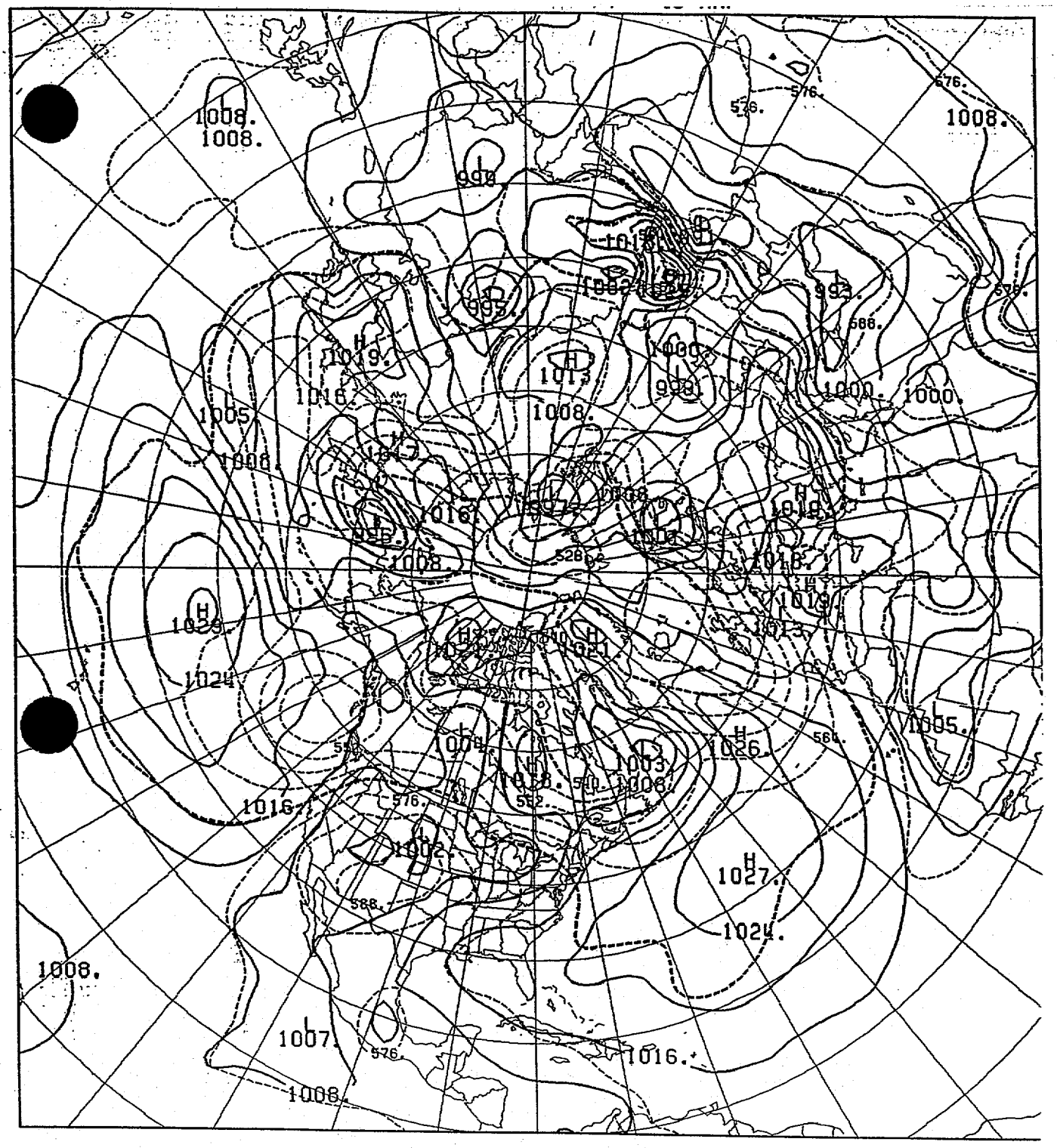
1008.
1008.
1008.
1008.
1008.
1008.
1008.
1008.
1007.
1016.
1016.
1016.
1019.
1019.
1019.
1013.
1013.
1000.
1000.
1000.
1005.
1005.
1024.
1024.
1024.
1027.
1026.
1003.
1004.
1002.
1016.
1016.
1018.
1018.
1019.
1019.
1021.
1021.
1029.
1013.
995.
993.
999.
576.
588.
528.
564.
552.
540.

fig 10

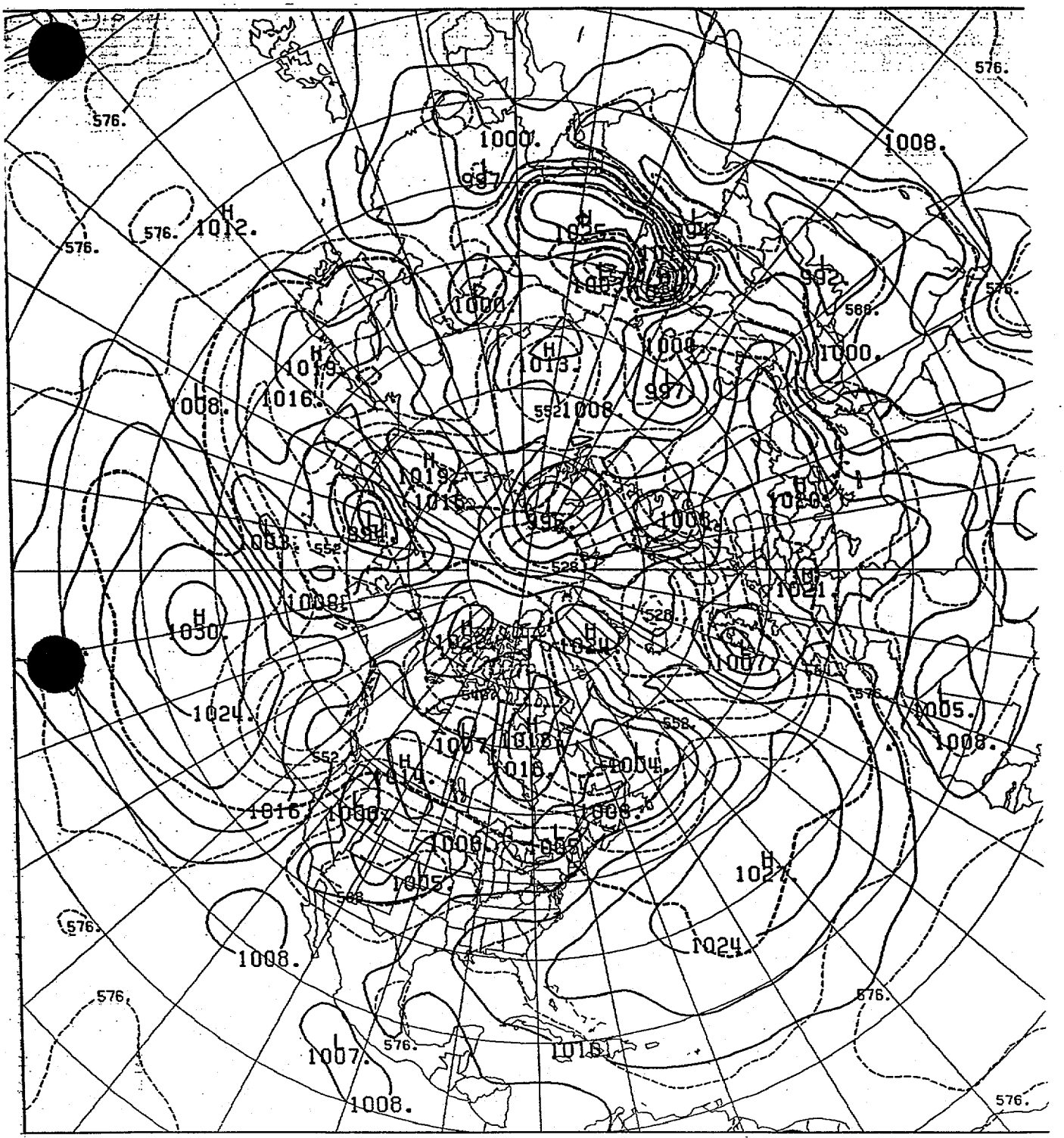
576.
1000.
1008.
1012.
1013.
1016.
1019.
1020.
1021.
1024.
1030.
1005.
1007.
1004.
1014.
1027.
1016.
997
992
994
1003.
552
528
568.

Fig 11

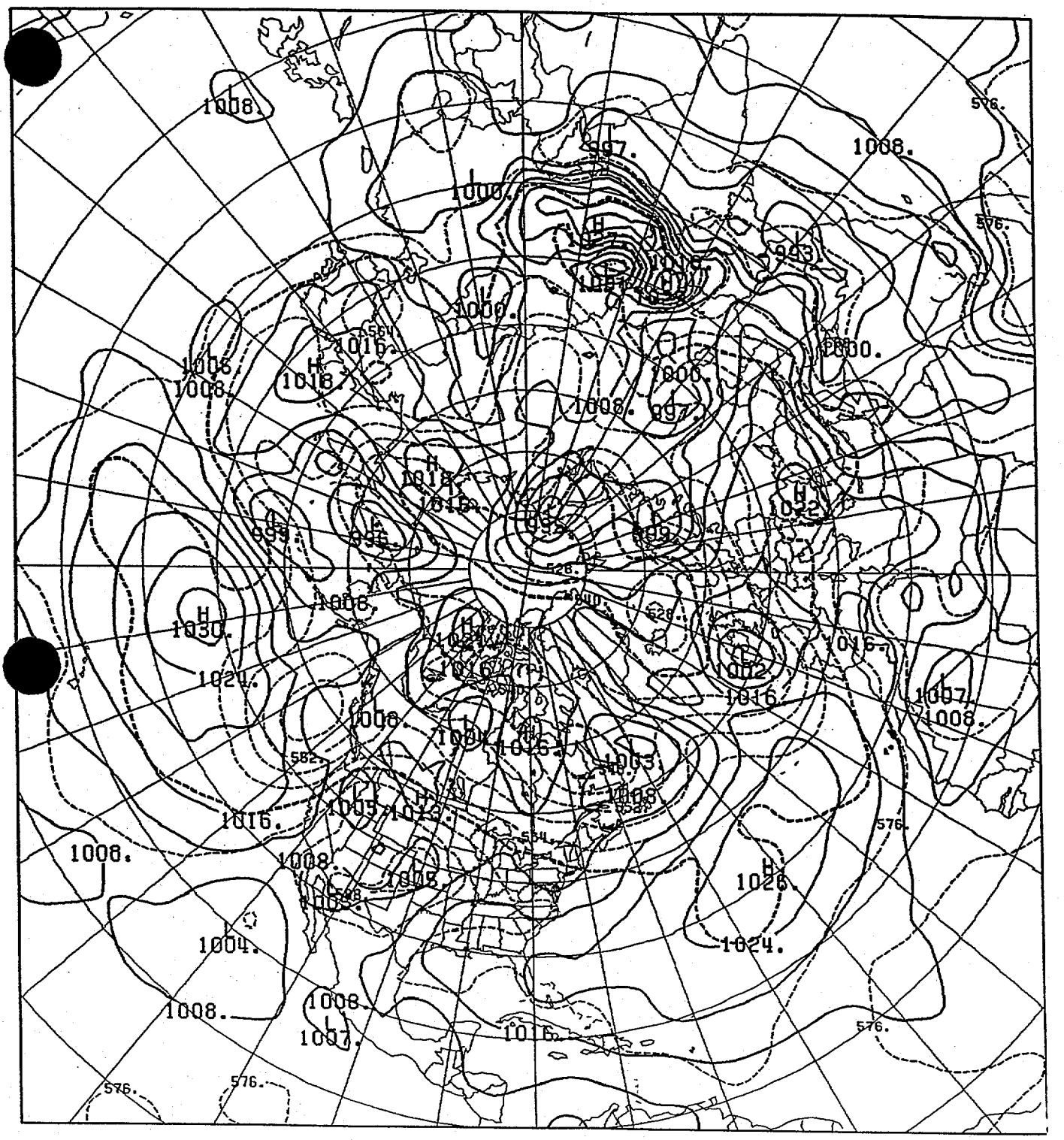
1008.
1000.
1016.
1018.
1030.
1024.
1004.
1007.
1026.
1003.
1022.
576.
564.
528.
552.

Fig 12

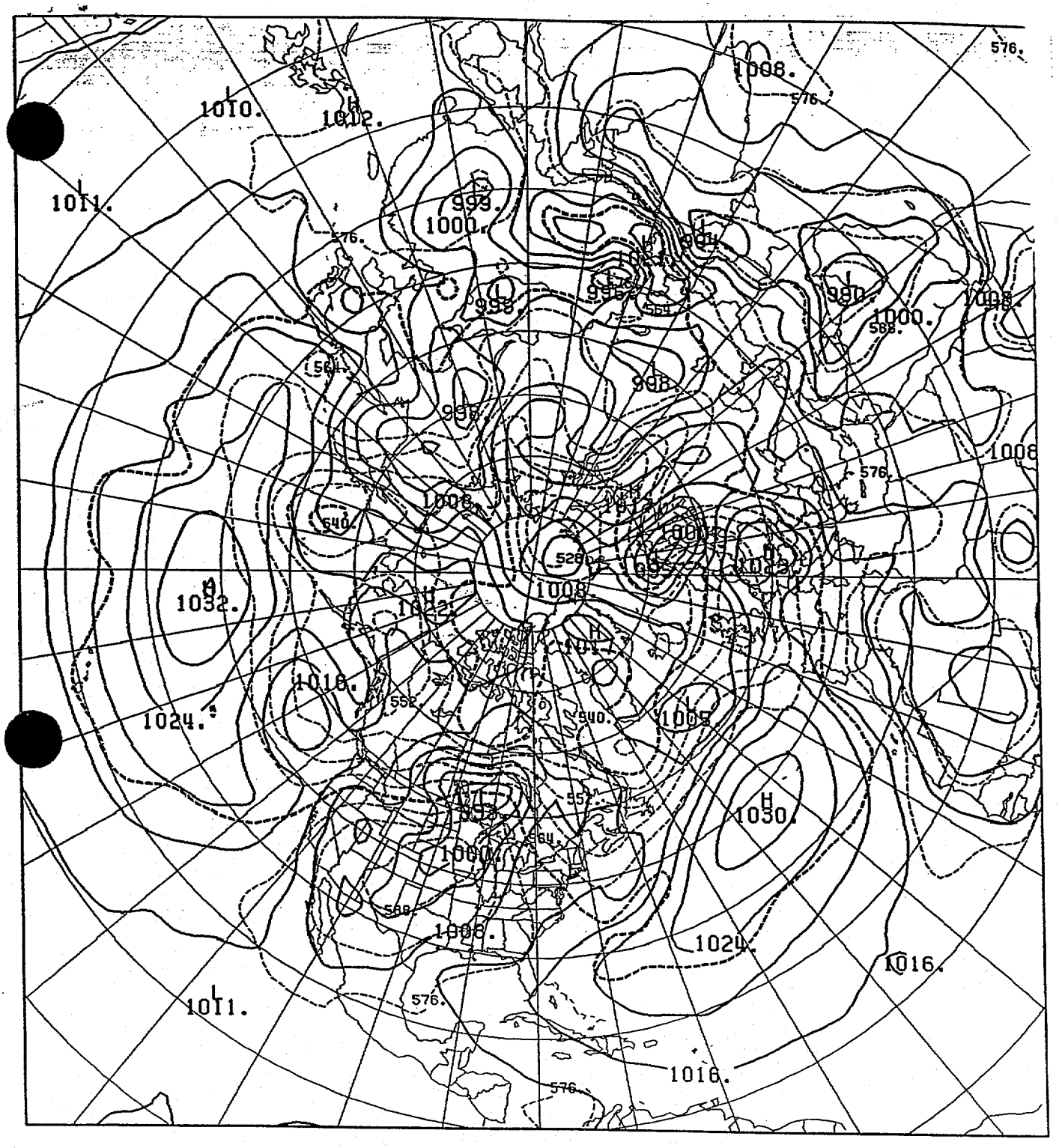
1010.
1012.
1011.
1008.
576.
999.
1000.
990.
1000.
1008.
998.
996.
1008
576.
1032.
1022.
1016.
1024.
1005.
1030.
1024.
1016.
1011.
576.
1016.
576.

Fig 13

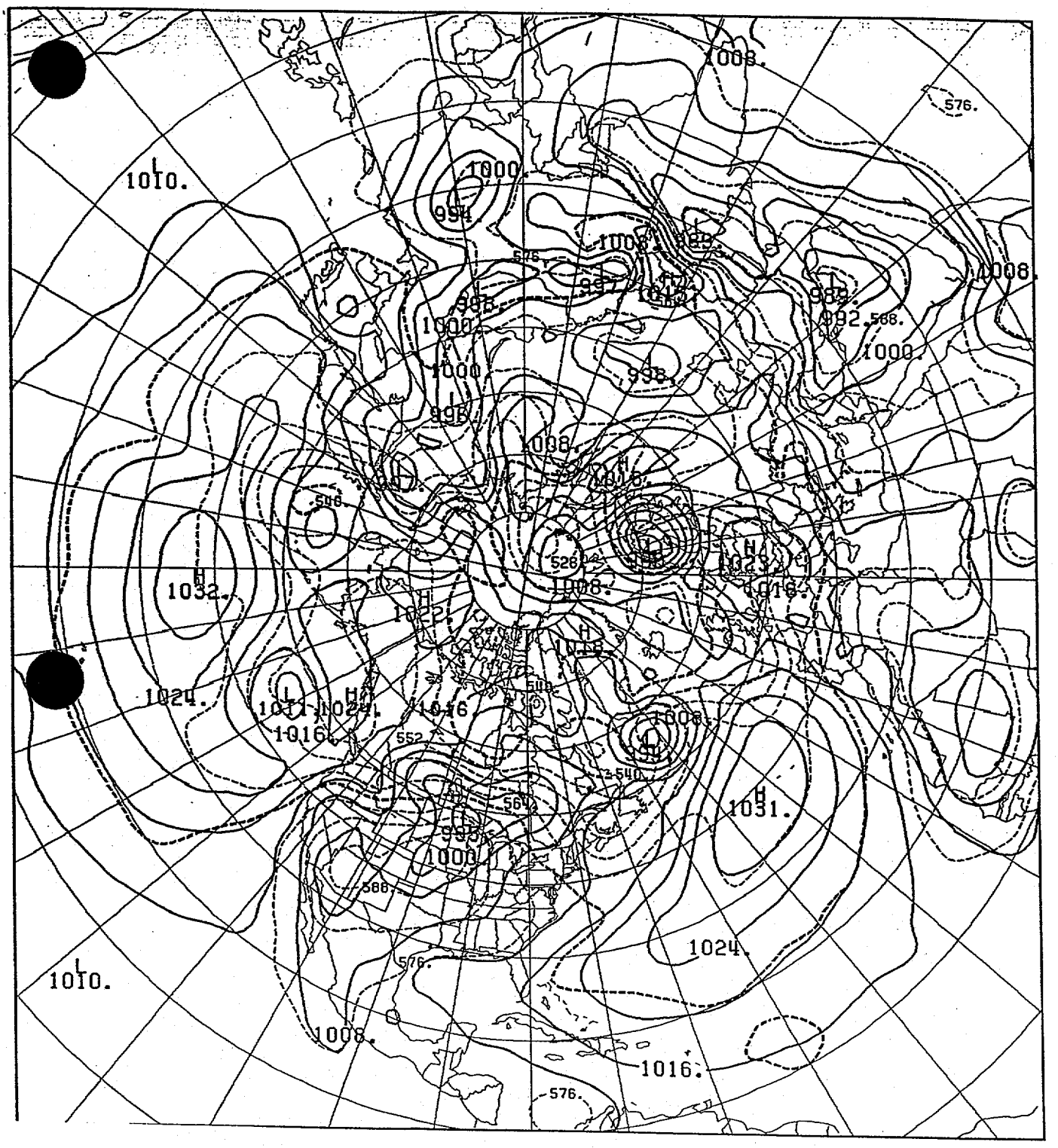
1008.
576.
1010.
1000.
994.
1008.
576.
1008.
992.
588.
1000.
1000.
998.
1008.
540.
528.
1008.
1032.
1022.
1016.
1024.
1016.
552.
540.
564.
1031.
1000.
588.
1024.
576.
1010.
1008.
1016.
576.

Fig 14

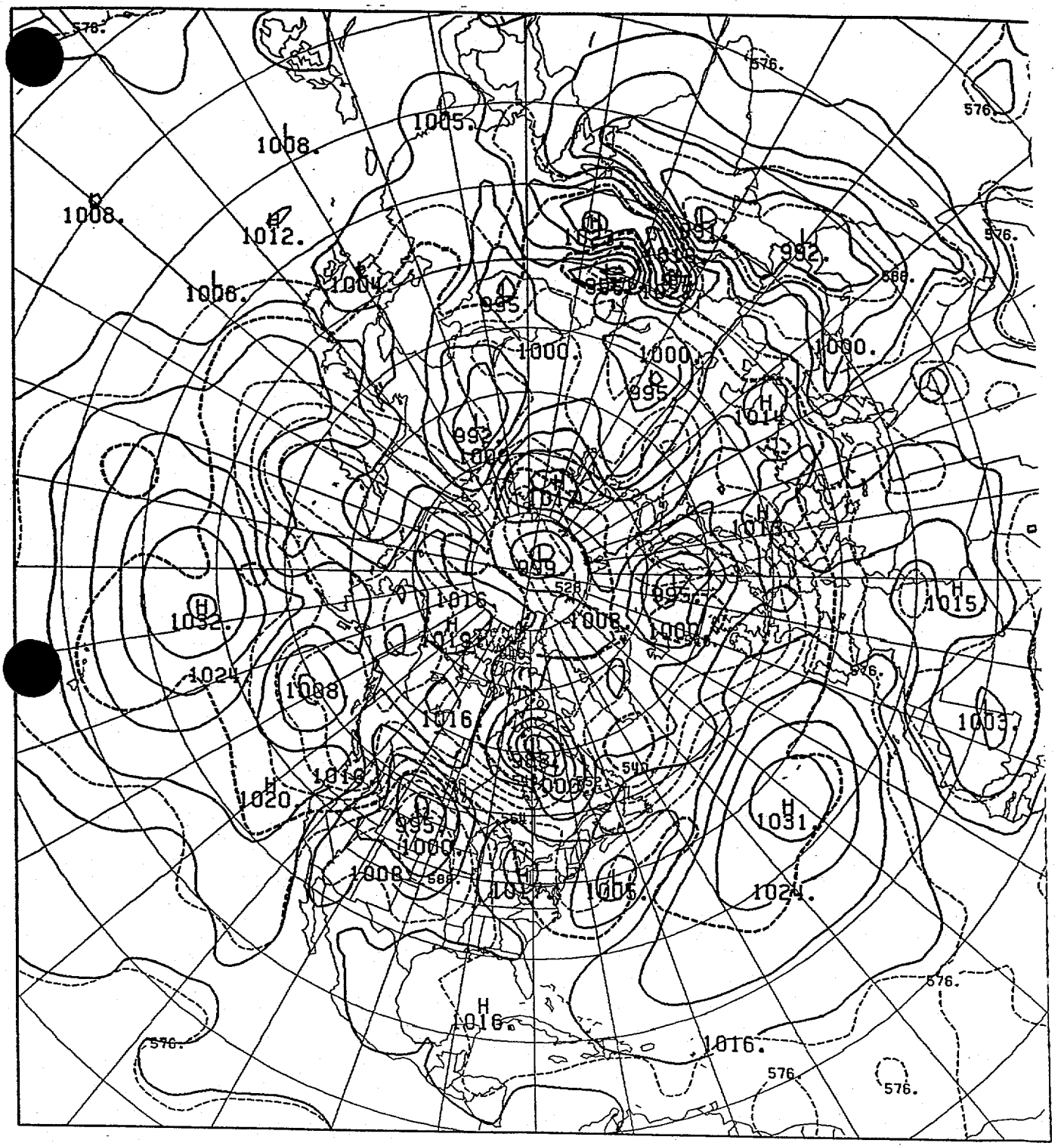
576.
1005.
1008.
1008.
1012.
1006.
1004.
995.
1000.
1000.
1000.
992.
995.
1014.
1032.
1024.
1008.
1016.
1015.
1003.
1020.
1031.
1024.
1016.
1016.
576.

Fig 15

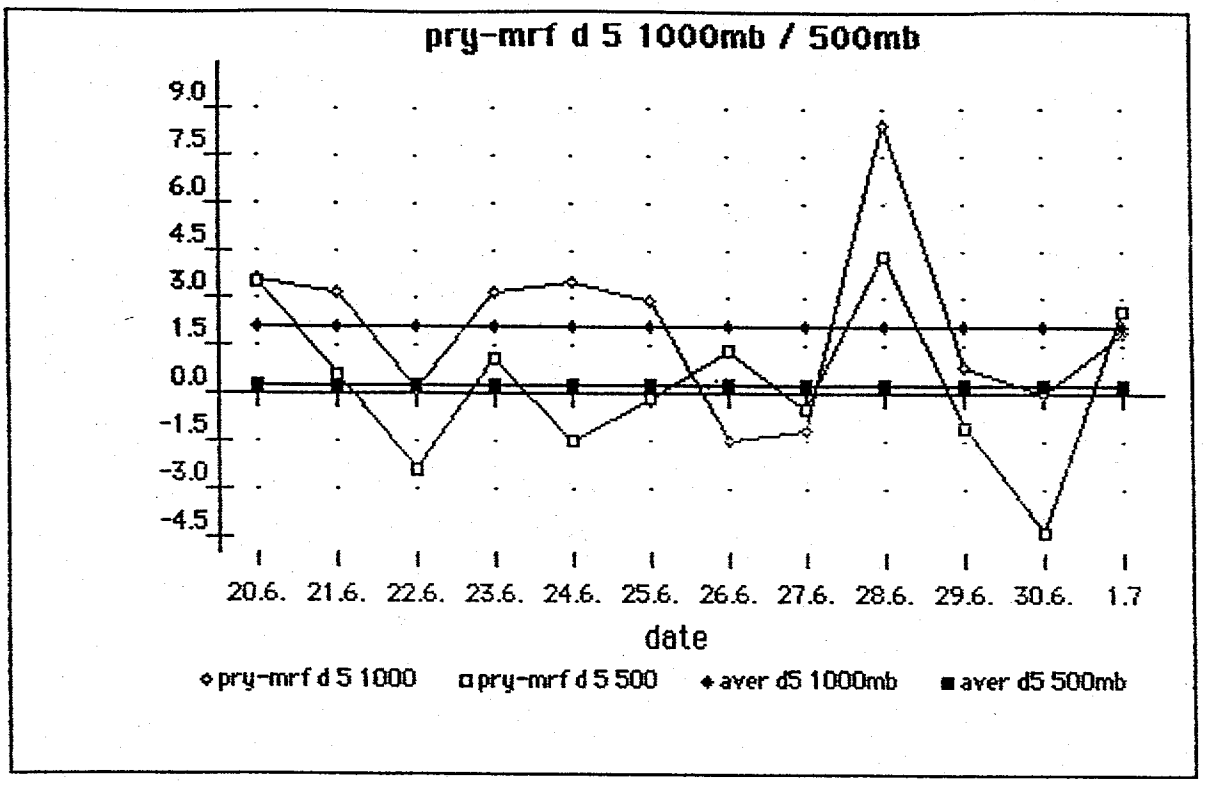
pry-mrf d 5 1000mb / 500mb
9.0
7.5
6.0
4.5
3.0
1.5
0.0
-1.5
-3.0
-4.5
20.6.
21.6.
22.6.
23.6.
24.6.
25.6.
26.6.
27.6.
28.6.
29.6.
30.6.
1.7
date
pry-mrf d 5 1000
pry-mrf d 5 500
aver d5 1000mb
aver d5 500mb

Fig 16